Letter

Direct measurement of dipoles in anomalous elasticity of amorphous solids

Bhanu Prasad Bhowmik,[1] Michael Moshe ,[2] and Itamar Procaccia[1,3]

[1]*Department of Chemical Physics, The Weizmann Institute of Science, Rehovot 76100, Israel*
[2]*Racah Institute of Physics, The Hebrew University of Jerusalem, Jerusalem 9190, Israel*
[3]*Center for Optical Imagery Analysis and Learning, Northwestern Polytechnical University, Xi'an 710072, China*

Recent progress in studying the physics of amorphous solids has revealed that mechanical strains can be strongly screened by the formation of plastic events that are typically quadrupolar in nature. The theory stipulates that gradients in the density of the quadrupoles act as emergent dipole sources, leading to strong screening and to qualitative changes in the mechanical response, as seen, for example, in the displacement field. In this Letter we first offer direct measurements of the dipole field, independently of any theoretical assumptions, and second we demonstrate detailed agreement with the recently proposed theory. These two goals are achieved by using data from both simulations and experiments. Finally, we show how measurements of the dipole fields pinpoint the theory parameters that determine the profile of the displacement field.

I. INTRODUCTION

Classical elasticity theory is one of the basic building blocks of condensed-matter physics. Once the elastic moduli of a given material are known [1], one can predict the displacement field that is associated with any mechanical strain [2] by using linear elasticity when the latter is small and applying nonlinear extensions of the theory when the strains are larger [3]. This happy state of affairs is, however, questioned when one studies the mechanical properties of amorphous solids. One reason is that, in amorphous solids, *plastic responses* appear instantaneously for any amount of strain [4]. Another reason is that nonlinear elastic constants were shown to have unbounded sample-to-sample fluctuations in the thermodynamic limit [5]. Finally, at least in frictional amorphous solids, one observes stress correlations that are not consistent with classical elasticity theory [6,7]. It is thus necessary to revisit elasticity theory in the context of amorphous solids with the aim of seeking an applicable theory that can provide predictive power.

Such a theory was presented in a recent paper [8]. Attention was given to the plastic responses, which typically appear as quadrupolar (Eshelby-like) irreversible responses [9–12]. When the density of these quadrupoles is low, they act only to renormalize the elastic moduli, but they do not change the form of the theory. This is reminiscent of the role of dipoles in dielectrics, where the dielectric constant is dressed, but the structure of electrostatic theory remains intact [13]. On the other hand, when the density of quadrupoles is high, the gradients of their density cannot be ignored, and these are acting as dipoles. Dipole-dipole and dipole-displacement interactions become crucial, and these change the structure of the theory and the resulting mechanical responses. Our main goal here is to directly measure the induced dipole density, independently of our previous theory.

II. BRIEF REVIEW OF THE THEORY

To introduce the theory in its simplest form we focus here on 2-dimensional systems with radial geometry. Specifically, we consider amorphous configurations of binary disks, with and without friction. For the frictionless case we examined in numerical simulations the displacement field that results from an inflation of a disk closest to the center. For the frictional case our collaborators studied experimentally the displacement field that is induced by a pusher at the center of coordinates whose effect is similar to the inflation considered *in silico*. Details of these simulations and experiments can be found in Refs. [8,14]. In short, in our experiment and simulations we consider an annulus of radii r_{in} and r_{out}, $r_{in} \ll r_{out}$, with an imposed displacement $\mathbf{d}(r_{in}) = d_0\hat{r}$ and $\mathbf{d}(r_{out}) = 0$. The polar symmetry of the problem implies that $\mathbf{d}(r) = d_r(r)\hat{r}$, in which case normal elasticity theory implies the equation

$$\Delta\mathbf{d} = d_r'' + \frac{d_r'}{r} - \frac{d_r}{r^2} = 0. \tag{1}$$

The solution to this differential equation that satisfies the boundary conditions is

$$d_r(r) = d_0 \frac{r^2 - r_{out}^2}{r_{in}^2 - r_{out}^2} \frac{r_{in}}{r}. \tag{2}$$

One should note that the solution (2) is a positive monotonically decreasing function of r, and it decays at large values of r like $1/r$, as expected in standard elasticity theory. It was shown [8] that this form of the displacement field is expected to remain valid also when there exists a low (or uniform) density of plastic events, although the coefficients may get renormalized. We then refer to this situation as "quasi-elastic."

The situation changes qualitatively when the density of plastic events gains sizable gradients, and these act as dipole

sources [8]. The screening caused by dipoles changes Eq. (2) to read

$$d_r'' + \frac{d_r'}{r} - \frac{d_r}{r^2} = -\kappa^2 d_r, \qquad (3)$$

with κ being an emergent constant that is not known *a priori*. Below we refer to κ as the "screening parameter." Equation (3) is equivalent to the Bessel equation whose solution, satisfying $d_r(r_{in}) = d_0$, $d_r(r_{out}) = 0$, reads

$$d_r(r) = d_0 \frac{Y_1(r\kappa)J_1(r_{out}\kappa) - J_1(r\kappa)Y_1(r_{out}\kappa)}{Y_1(r_{in}\kappa)J_1(r_{out}\kappa) - J_1(r_{in}\kappa)Y_1(r_{out}\kappa)}. \qquad (4)$$

Here J_1 and Y_1 are the Bessel functions of the first and second kind, respectively. For very small values of κ the solution reduces back to (2). Importantly, depending on the precise value of κ, Eq. (4) may be nonmonotonic, negative, and even oscillatory. We refer to situations that agree with the solution (4) and are either nonmonotonic or oscillating as "anomalous elasticity." Until now the numerical values of κ had to be determined by fitting Eq. (4) to experiments and simulations [8,14]. A consequence of the present Letter will be a direct determination of the screening parameter κ, as shown below.

Two examples for further analysis

Our next aim is to establish the existence (or nonexistence) of dipole fields, directly from the measured displacement field. We choose two examples, the first being a numerical simulation of frictionless binary amorphous assembly of disks [8], and the second an experiment with frictional binary disks [14], all in circular geometry, and both showing anomalous responses. The displacement fields in these cases result from an inflation of a disk or a pusher at the center of coordinates. The angle-averaged radial component of the displacement field as measured in a simulation and an experiment respectively are shown in Fig. 1. Both examples deviate strongly from the elastic solution (2). Rather, the continuous lines in both panels represent the anomalous solutions (4) with κ being a fitting parameter. Figures 1(a) and 1(b) are obtained with $\kappa = 0.0525$ and $\kappa = 0.00147$, respectively. We note here that the systems are of different sizes and κ is dimensional. For the sake of comparison one should consider a dimensionless number $\tilde{\kappa} \equiv \kappa r_{out}$. Then the two examples have $\tilde{\kappa} = 3.79$ and 5.11, respectively. One of our goals below is to develop a direct measure for the screening parameter κ and to test its success in predicting the curves in Fig. 1, without fitting.

III. THEORY-INDEPENDENT MEASUREMENT OF DIPOLES

A. Technical preliminaries

To set up the direct measurement of dipoles, we start with the most general energy functional constructed to describe a screening mechanism in a domain Ω of an elastic solid:

$$F = \int_\Omega W_{el}\, dS + \int_\Omega W_{sc}\, dS - \oint t^\alpha d_\alpha\, dS, \qquad (5)$$
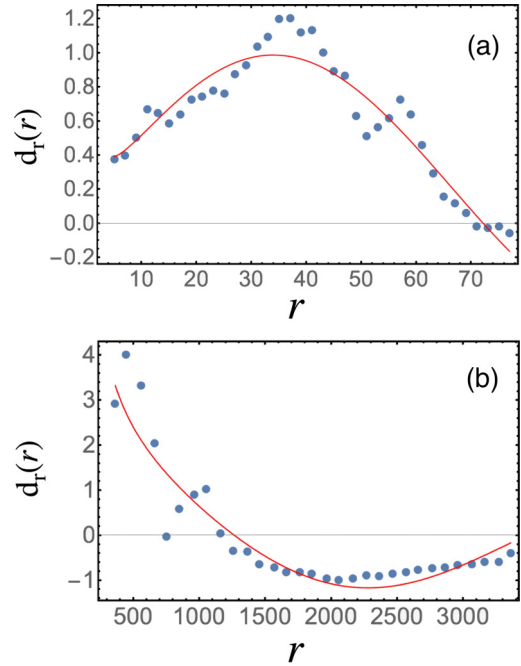

FIG. 1. Angle-averaged radial components of the displacement field as measured in simulation and experiment, cf. Refs. [8,14]. Panel (a) shows simulations with frictionless Hertzian disks, exhibiting an anomalous response. The continuous line is the solution Eq. (4) with $r_{in} = 4.8$, $r_{out} = 72.2$, and $\kappa = 0.0525$. Panel (b) shows experimental measurements with frictional disks, The continuous line is the solution Eq. (4) with $r_{in} = 133.3$, $r_{out} = 3478$, and $\kappa = 0.001\,47$.

with elastic and screening contributions to the energy

$$W_{el} = \frac{1}{2} A^{\alpha\beta\gamma\delta} u_{\alpha\beta} u_{\gamma\delta},$$

$$W_{sc} = \frac{1}{2} A^{\alpha\beta\gamma\delta} u_{\alpha\beta} \mathcal{F}^{(1)}_{\gamma\delta}(Q) + \mathcal{F}^{(2)}(Q). \qquad (6)$$

Here $\mathcal{F}^{(1)}$ and $\mathcal{F}^{(2)}$ are functions of an emergent quadrupole field Q and its derivative, the first traceless and the second positive definite. The traction force on the boundary is **t**. We assume emergent quadrupoles since these are the basic plastic events that are pertinent to the mechanics of amorphous solids.

Next we compute the variation of the energy functional with respect to displacement field **d**:

$$\delta F = -\int \partial_\alpha \big(\sigma^{\alpha\beta} + A^{\alpha\beta\gamma\delta}\mathcal{F}^{(1)}_{\gamma\delta}\big)\delta d_\beta\, dS$$

$$+ \oint \big(\sigma^{\alpha\beta} + A^{\alpha\beta\gamma\delta}\mathcal{F}^{(1)}_{\gamma\delta}\big)\hat{n}_\alpha \delta d_\beta\, dl$$

$$- \oint t^\alpha \delta d_\alpha\, dS. \qquad (7)$$

Denote now $\Sigma^{\alpha\beta} = \sigma^{\alpha\beta} + A^{\alpha\beta\gamma\delta}\mathcal{F}^{(1)}_{\gamma\delta}$ and observe that the variation vanishes at equilibrium, leading to

$$\partial_\alpha \Sigma^{\alpha\beta} = 0, \quad \Sigma^{\alpha\beta} n_\alpha|_{boundary} = t^\beta. \qquad (8)$$

Σ is therefore the physical stress tensor. Being divergentless, it can always be written in terms of an Airy function χ,

$$\Sigma^{\alpha\beta} = \epsilon^{\alpha\mu}\epsilon^{\beta\nu}\partial_{\mu\nu}\chi. \tag{9}$$

The pressure is therefore

$$p \equiv \mathrm{Tr}\Sigma = \Delta\chi. \tag{10}$$

From the relation between the physical stress Σ and the coupling tensor $F^{(1)}$ we get

$$u_{\rho\sigma} = A_{\rho\sigma\alpha\beta}\epsilon^{\alpha\mu}\epsilon^{\beta\nu}\partial_{\mu\nu}\chi - \mathcal{F}^{(1)}_{\rho\sigma}. \tag{11}$$

And from geometric compatibility condition we get

$$-\frac{1}{Y}\Delta\Delta\chi = \nabla_{\alpha\beta}q^{\alpha\beta}, \quad q^{\alpha\beta} \equiv \epsilon^{\alpha\mu}\epsilon^{\beta\nu}\mathcal{F}^{(1)}_{\mu\nu}, \tag{12}$$

where Y is the Young's modulus. Finally, denote $\nabla_\beta q^{\alpha\beta} \equiv -P^\alpha$. Since the divergence of a quadrupole density is identically the dipole density, we refer to the existence of the vector field P as a case of emergent dipoles. Next we ask how can we ascertain whether P exists from the displacement data.

B. Measurement of the dipole field

We have shown in the last section that emergent dipoles are introduced as sources for the biharmonic equation for the Airy function [15]. We thus can start with this equation in the form [16–19]

$$\frac{1}{Y}\Delta\Delta\chi = \nabla \cdot \mathbf{P}, \tag{13}$$

with $\mathbf{P}(x)$ being the position-dependent dipole density. Using Eq. (10), we compute the integral of the left-hand side (LHS) of Eq. (13) over a domain Ω:

$$\frac{1}{Y}\int_\Omega \Delta\Delta\chi \, dS = \frac{1}{Y}\oint_{\partial\Omega}(\nabla\Delta\chi)\cdot\mathbf{n}\,dl = \frac{1}{Y}\oint_{\partial\Omega}(\nabla p)\cdot\mathbf{n}\,dl, \tag{14}$$

where n is the outgoing unit vector on the boundary of the domain. On the other hand, the integral of the right-hand side (RHS) of Eq. (13) reads

$$\int_\Omega \nabla \cdot \mathbf{P}\, dS = \oint_{\partial\Omega}\mathbf{P}\cdot\mathbf{n}\,dl. \tag{15}$$

We therefore conclude that the signature for the existence of nonuniform dipole distribution is from the integral over the pressure flux

$$\frac{1}{Y}\oint_{\partial\Omega}(\nabla p)\cdot\mathbf{n}\,dl = \oint_{\partial\Omega}\mathbf{P}\cdot\mathbf{n}\,dl. \tag{16}$$

Note that the pressure is proportional to the trace of the strain $p = Y\,\mathrm{Tr}(u)$, which in turn describes the volume deformation of the material and is equal to the displacement divergence $\mathrm{Tr}(u) = \nabla \cdot d$. Denoting the resulting integral as I_1 we end up with

$$\oint_{\partial\Omega}\mathbf{P}\cdot\mathbf{n}\,dl = \oint_{\partial\Omega}(\nabla(\nabla \cdot \boldsymbol{d}))\cdot\mathbf{n}\,dl \equiv I_1. \tag{17}$$

In the case of our circular systems with radial symmetry both sides of this equation can be evaluated analytically. The RHS
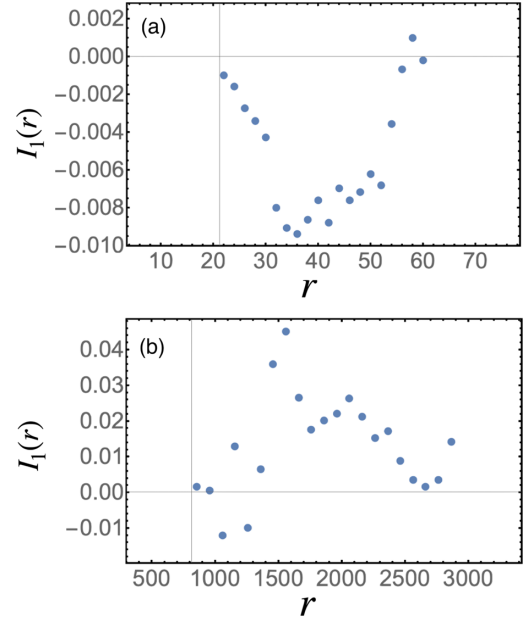

FIG. 2. The integral I_1 of Eq. (18) computed for the two anomalous examples shown in panels (a) and (b) of Fig. 1. These plots use the data without any resort to theoretical fits. The existence of these integrals are a direct demonstration for the presence of dipole fields.

reads

$$\oint_{\partial\Omega}(\nabla(\nabla \cdot \boldsymbol{d}))\cdot\mathbf{n}\,dl = 2\pi r\left(d_r''(r) + \frac{d_r'(r)}{r} - \frac{d_r(r)}{r^2}\right), \tag{18}$$

and the LHS reads

$$\oint_{\partial\Omega}\mathbf{P}\cdot\mathbf{n} = 2\pi r P(r), \tag{19}$$

hence

$$P(r) = d_r''(r) + \frac{d_r'(r)}{r} - \frac{d_r(r)}{r^2}. \tag{20}$$

We should notice that Eq. (1) guarantees that the expression for the dipole density in Eq. (20) is zero identically when classical elasticity is obeyed. Since this is correct for every closed circle, it means that $P(r) = 0$. This is consistent with the absence of dipole sources. Note also that in two dimensions the elasticity theory solution for the radial component of the displacement field, being proportional to $1/r$ at large values of r results in a trivial zero on the RHS of Eq. (18).

At this point we return to the two examples shown in Fig. 1 and compute the dipole density in Eq. (20) directly from the measured radial component. The results for the frictionless simulation and the frictional experiment are shown in Fig. 2. Although the data are somewhat noisy, we can see that the measured dipole density is nonzero for the two cases, indicating that, indeed, dipole sources exist in the system, as they emerge together with the onset of the displacement fields. We stress that this result is independent of the theory proposed in Ref. [8]. A theory-dependent fit to Eq. (4) yields a smoother measure for I_1. The result is shown for the two examples in Fig. 3. The two methods of evaluation are consistent with each other and show that a dipole field is emerging together with
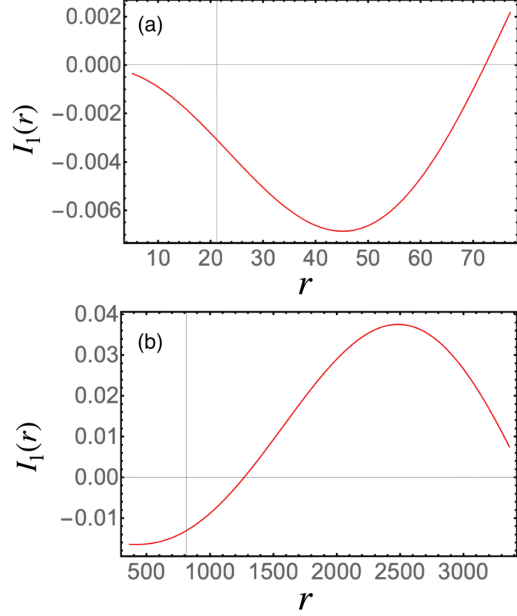
FIG. 3. The same integral I_1 of Eq. (18) computed for the two examples shown in Fig. 1. Here we use the fit Eq. (4) for the sake of smoothness. These integrals are identical to those obtained using Eq. (23) up to the scale κ^2, as is demanded from the solution Eq. (4).

the displacement field which is caused by the inflation near the center of our amorphous solids in their radial geometry.

C. Theory-dependent evaluation

Next we test the theory that was proposed in Ref. [8] where an anomalous response of the system is described by Eq. (3):

$$\nabla \mathrm{Tr}(u) = (\nabla(\nabla \cdot \boldsymbol{d})) = -\kappa^2 \mathbf{d}, \qquad (21)$$

hence the integrand in LHS of Eq. (18) can be simplified,

$$\oint_{\partial\Omega} \mathbf{P} \cdot \mathbf{n}\, dl = -\kappa^2 \oint_{\partial\Omega} \mathbf{d} \cdot \mathbf{n}\, dl. \qquad (22)$$

If the theory is correct, the evaluation using the RHS of Eq. (22) should agree with the evaluation of Eq. (18). Denote the integral itself as I_2,

$$I_2 \equiv -\oint_{\partial\Omega} \mathbf{d} \cdot \mathbf{n}\, dl. \qquad (23)$$

Since we have used in Fig. 3 the solution of Eq. (4) to compute I_1, it is obvious that I_2 would be identical to I_1 up to the scale factor κ^2. Computing $\sqrt{I_1/I_2}$ one indeed finds the evident value of κ which was used to fit the data in Fig. 1.

Thus far we did not put the theory of Ref. [8] under a stringent test. To achieve such a test we return to the raw data of the angle averaged displacements shown in Fig. 1. To avoid effects of noise we smooth the displacement data by calculating moving averages. The displacement at each position r is estimated from the average of eight nearest neighbors. In addition, we note that the integrals $I_{1,2}$ measure the dipole *density* $P(r)$. Upon integrating over the radial direction we
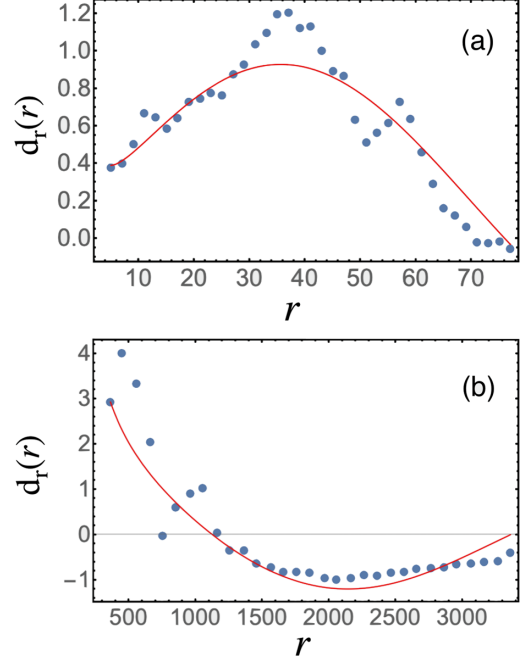

FIG. 4. Comparison of the solutions obtained using the screening parameter κ from the measurements of the dipole fields. Panel (a) shows a comparison with the experimental data (blue points) as shown in Fig. 1(a). Panel (b) shows a comparison with the simulation data (blue points) shown in Fig. 1(b).

find the total dipole charge induced in the system

$$\begin{aligned}
\mathcal{P}_{\mathrm{tot}} &= 2\pi \int rP(r)dr \\
&= \kappa^2 \int I_2(r)dr = \int I_1(r)dr.
\end{aligned} \qquad (24)$$

Therefore we can estimate κ by

$$\kappa = \sqrt{\frac{\int I_1(r)dr}{\int I_2(r)dr}}. \qquad (25)$$

This ratio can be calculated directly from the raw data. We find the values $\kappa = 0.049\,80$ and $\kappa = 0.001\,46$ for the two examples in Fig. 1. If the theory is correct, when these measured values of κ are plugged into the predicted form in Eq. (4) the resulting curves should agree with the measured radial components of the displacement without performing any fitting procedure. Indeed, in Fig. 4 we plot the predicted form (4) and the measured displacement using the calculated κ and find very good agreement, thus providing a support to the dipole screening picture in general and to our specific model in particular.

IV. SUMMARY AND CONCLUSIONS

The aim of this Letter was twofold. First we wanted to present a direct computation of the dipole field that was presumed to exist in Refs. [8,14]. Contrary to the case of electrostatics [13], where dipoles can be directly attributed to polarized molecules or polymers, in the present case dipoles were identified as gradients of quadrupole fields, rendering

them less obvious. We have shown in this Letter how to compute the dipole fields from loop integrals on the displacement field. The existence of a dipole field goes hand in hand with a finite value of the screening parameter κ and with having anomalous elasticity. *Mutatis mutandis*, when $\kappa = 0$ we expect quasi-elastic responses with a possible renormalization of the elastic moduli.

The second aim of this Letter was to present a method to estimate the numerical value of the screening parameter κ from the measurement of the dipole field. The total dipole charge, as defined in Eq. (24), provides us with a method to compute κ from Eq. (25), without fitting the angle-averaged displacement field. The agreement of the prediction of Eq. (4) with the data, once we used the screening parameter from this procedure, is strong support for the theory as presented in Refs. [8,14].

It should be stated that until now the theory was tested by and compared with simulations and experiments involving disks in radial geometry in two dimensions. In the near future we will provide evidence that the theory is also applicable to systems of spheres in three dimensions and to standard models of glass formers in two and three dimensions.

[1] J. F. Lutsko, Generalized expressions for the calculation of elastic constants by computer simulation, J. Appl. Phys. **65**, 2991 (1989).

[2] L. D. Landau and E. M. Lifshitz, *Theory of Elasticity, Third Edition*, Course of Theoretical Physics (Butterworth-Heinemann, Oxford, 1986), Vol. 7.

[3] J. Cassels, N. Hitchin *et al.*, *Nonlinear Elasticity: Theory and Applications* (Cambridge University Press, Cambridge, UK, 2001).

[4] S. Karmakar, E. Lerner, and I. Procaccia, Athermal nonlinear elastic constants of amorphous solids, Phys. Rev. E **82**, 026105 (2010).

[5] H. G. E. Hentschel, S. Karmakar, E. Lerner, and I. Procaccia, Do athermal amorphous solids exist? Phys. Rev. E **83**, 061101 (2011).

[6] A. Lemaître, C. Mondal, I. Procaccia, and S. Roy, Stress correlations in frictional granular media, Phys. Rev. B **103**, 054110 (2021).

[7] A. Lemaître, C. Mondal, I. Procaccia, S. Roy, Y. Wang, and J. Zhang, Frictional Granular Matter: Protocol Dependence of Mechanical Properties, Phys. Rev. Lett. **126**, 075501 (2021).

[8] A. Lemaître, C. Mondal, M. Moshe, I. Procaccia, S. Roy, and K. Screiber-Re'em, Anomalous elasticity and plastic screening in amorphous solids, Phys. Rev. E **104**, 024904 (2021).

[9] J. D. Eshelby, The determination of the elastic field of an ellipsoidal inclusion, and related problems, Proc. R. Soc. London, Ser. A **241**, 376 (1957).

[10] D. L. Malandro and D. J. Lacks, Relationships of shear-induced changes in the potential energy landscape to the mechanical properties of ductile glasses, J. Chem. Phys., **110**, 4593 (1999).

[11] C. E. Maloney and A. Lemaître, Amorphous systems in athermal, quasistatic shear, Phys. Rev. E **74**, 016118 (2006).

[12] M. Baggioli, I. Kriuchevskyi, T. W. Sirk, and A. Zaccone, Plasticity in Amorphous Solids is Mediated by Topological Defects in the Displacement Field, Phys. Rev. Lett. **127**, 015501 (2021).

[13] L. Landau and E. Lifshitz, *Electrodynamics of Continuous Media*, 2nd ed. (Pergamon Press, Oxford, 1984), Chap. 1.

[14] C. Mondal, M. Moshe, I. Procaccia, S. Roy, J. Shang, and J. Zhang, Anomalous elasticity in frictional matter, arXiv:2108.13334.

[15] N. Muskhelishvili, *Some Basic Problems of the Mathematical Theory of Elasticity* (Springer Science & Business Media, Netherlands, 2013).

[16] M. Moshe, E. Sharon, and R. Kupferman, Elastic interactions between two-dimensional geometric defects, Phys. Rev. E **92**, 062403 (2015).

[17] W. T. Irvine, V. Vitelli, and P. M. Chaikin, Pleats in crystals on curved surfaces, Nature (London) **468**, 947 (2010).

[18] S. Sarkar, M. Čebron, M. Brojan, and A. Košmrlj, Elastic multipole method for describing deformation of infinite two-dimensional solids with circular inclusions, Phys. Rev. E **103**, 053003 (2021).

[19] S. Sarkar, M. Čebron, M. Brojan, and A. Košmrlj, Method of image charges for describing deformation of bounded two-dimensional solids with circular inclusions, Phys. Rev. E **103**, 053004 (2021).